

THE CANADIAN MINERALOGIST

JOURNAL OF THE MINERALOGICAL ASSOCIATION OF CANADA

Volume 42

February 2004

Part 1

The Canadian Mineralogist
Vol. 42, pp. 1-16 (2004)

THE COEXISTENCE OF MELTS OF HYDROUS COPPER CHLORIDE, SULFIDE AND SILICATE COMPOSITIONS IN A MAGNESIOHASTINGSITE CUMULATE, TUBAF SEAMOUNT, PAPUA NEW GUINEA

AXEL D. RENNO[§] AND LEANDER FRANZ

Institut für Mineralogie, TU Bergakademie Freiberg, Brennhausgasse 14, D-09596 Freiberg, Germany

THOMAS WITZKE

Institut für Mineralogie und Lagerstättenlehre, RWTH Aachen, Willnerstr. 2, D-52056 Aachen, Germany

PETER M. HERZIG

Institut für Mineralogie, TU Bergakademie Freiberg, Brennhausgasse 14, D-09596 Freiberg, Germany

ABSTRACT

Direct evidence for a Cu-Cl-salt-hydrate melt in equilibrium with a complex system of silicate melts was found in a xenolith of magnesiohastingsite-dominant cumulate from the TUBAF Seamount, near Lihir Island, in Papua New Guinea. The cumulate formed less than 1.5 Ma ago in a magma chamber in the oceanic crust. Petrographic observations give evidence for the coexistence of two different silicate melts, a Cu-Fe-S melt, the salt-hydrate melt and a vapor phase as an intercumulus assemblage. The salt-hydrate melt crystallized to clinoatacamite, whereas the only mineral crystallizing from the silicate melt was hydroxylapatite. The two observed silicate melts are of trachyandesitic-tephriphonolitic and foiditic composition, clearly different from the trachybasaltic host-magma. Exsolution of the Cu-Fe-S melt likely took place in the temperature range between 960° and 557°C. Its chemical composition ranges between chalcopyrite and intermediate solid-solution (*Iss*). On the basis of experimental data of other salt-hydrate – silicate melt systems, the unmixing of the Cu-Cl-salt-hydrate melt must have taken place below 800°C. This unmixing demonstrates how metal-enriched magmatic fluids can enter pre-existing hydrothermal systems.

Keywords: Cu-Cl-salt-hydrate melt, liquid immiscibility, clinoatacamite, ore-forming processes, TUBAF Seamount, Papua New Guinea.

SOMMAIRE

Nous décrivons un exemple d'un bain fondu à composition d'un oxyseil Cu-Cl hydraté en équilibre avec un système silicaté complexe dans un fragment de cumulat xénolithique à dominance de magnésiohastingsite provenant du guyot de TUBAF, près de l'île de Lihir, en Papouasie – Nouvelle Guinée. Le cumulat se serait formé il y a moins de 1.5 Ma dans une chambre magmatique dans la croûte océanique. Nos observations pétrographiques démontrent la coexistence de deux liquides silicatés différents, un liquide Cu-Fe-S, le bain fondu à composition de l'oxyseil de cuivre hydraté, et une phase vapeur dans l'assemblage intercumulatif.

[§] E-mail address: axel.renno@mineral.tu-freiberg.de

Ce bain fondu inhabituel a cristallisé en clinooatamite, tandis que le seul minéral à cristalliser à partir du liquide silicaté était l'hydroxylapatite. Les deux liquides silicatés ont une composition trachyandésitique-tephriphonolitique et foïditique, et diffèrent nettement de la composition du magma encaissant, trachybasaltique. L'exsolution du liquide Cu-Fe-S a probablement eu lieu dans l'intervalle de température entre 960° et 557°C. Sa composition chimique varie entre celle de la chalcopryrite et une solution solide intermédiaire (*Iss*). Compte tenu des données expérimentales sur d'autres systèmes contenant une coexistence de bain fondu à composition d'oxysel hydraté et de liquide silicaté, nous croyons que la démixion de liquide à oxysel Cu-Cl hydraté a eu lieu à une température inférieure à 800°C. Cette démixion démontre comment un fluide magmatique enrichi en métaux peut s'insérer dans un système hydrothermal pré-existant.

(Traduit par la Rédaction)

Mots-clés: bain fondu à oxysel Cu-Cl hydraté, immiscibilité liquide, clinooatamite, processus de minéralisation, guyot de TUBAF, Papouasie – Nouvelle Guinée.

INTRODUCTION

Traditionally, both Cu-S and Cu-Cl aqueous complexes are described as the main agents of mobilization, transport and concentration of copper during the formation of various kinds of ore deposits (*e.g.*, Barnes 1979, Ruaya & Seward 1986, Bischoff & Rosenbauer 1987). However, Earth scientists seldom can observe the generation and transport of these compounds directly. Exceptional circumstances in geological systems in some cases reveal the course of such events. Here, we present the results of our investigations of a salt hydrate melt, which developed in equilibrium with a complex system consisting of two silicate melts, a Cu-Fe sulfide melt, and a volatile phase. All these phases are hosted in a clin amphibole cumulate xenolith, which was transported to the seafloor in a trachybasaltic magma. The cumulate formed in the magma chamber of the TUBAF Seamount, Bismarck Archipelago, Papua New Guinea. The sudden recharge of this magma chamber by a new pulse of magma led to the fast uprising of cumulate xenoliths and preserved the observed salt-hydrate melt as clinooatamite. Our observations clearly attest to a primary origin of the melts in the cumulate, which formed by liquid immiscibility processes during cooling.

GEOLOGICAL SETTING

The TUBAF Seamount is part of the Tabar – Lihir – Tanga – Feni volcanic island chain, northeast of New Ireland in the Bismarck Archipelago (Fig. 1). The Bismarck Archipelago is located northeast of Papua New Guinea and includes the islands of New Britain, New Ireland – New Hanover, Bougainville and the Solomons. The plate-tectonic situation in this area involves southward subduction of the Pacific plate beneath the Bismarck microplate at the Manus – Kilinailau trench. The subduction triggered voluminous calc-alkaline arc volcanism during the Oligocene and Miocene. About 15 million years ago, the trench was blocked by its collision with the Ontong – Java plateau (Coleman & Kroenke 1981). Plate rotation, stress relocation, and a change in the direction of subduction were the direct

consequences of this blockage. Today, the Solomon Sea microplate is being subducted under the Bismarck microplate, forming the NNW–NNE-dipping New Britain trench.

The Tabar – Lihir – Tanga – Feni chain of volcanic islands extends for a distance of more than 260 km northeast of New Ireland. The volcanic activity started about 3 Ma ago on the island of Simberi, which belongs to the group of Tabar Island (Rytuba *et al.* 1993). The high-K calc-alkaline volcanism seems to be related to lithospheric extension along northeast-trending faults (Stracke & Hegner 1998), which were generated during the opening of the Manus back-arc basin (Taylor 1979, Kennedy *et al.* 1990). The thinning of the lithosphere under the New Ireland basin led to adiabatic decompression-induced melting of the underlying mantle regions and to the production of the magmas described above (McInnes & Cameron 1994).

In the course of three cruises with the R.V. Sonne (SO-94, SO-133 and SO-166), twelve submarine volcanos were detected near Lihir Island with the help of the hydrosweep sonar method. These volcanos were sampled using a dredge and a video-guided grab (Herzig *et al.* 1994, 1998). The samples from the TUBAF volcano were found to contain abundant xenoliths from the underlying mantle and from the oceanic crust (McInnes *et al.* 1999, 2001, Franz *et al.* 2002). Sample 54GTV2P, hereafter 54-2P, a clin amphibole-dominant cumulate, is the subject of this study.

PETROGRAPHIC OBSERVATIONS

The sample studied is an unusual xenolith of about 3 cm in diameter, hosted by a Quaternary trachybasalt. The trachybasalt displays a porphyritic texture with mm-sized crystals of clin amphibole, flakes of phlogopite and minor plagioclase in a fine-grained matrix consisting of a spinel phase, clin amphibole, plagioclase and devitrified glass. Furthermore, numerous mm-sized xenocrysts of olivine and clinopyroxene are present.

What makes the xenolith most unusual is the presence of domains of clinooatamite in the glass matrix. Based on its texture and according to the nomenclature

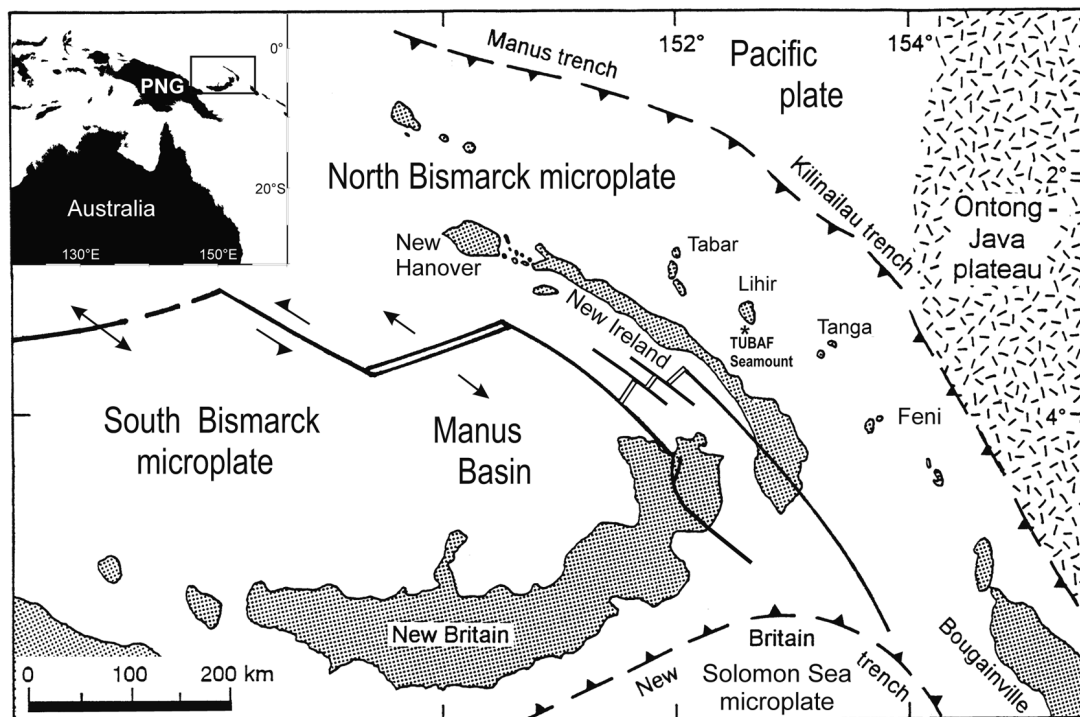


FIG. 1. Map of the plate-tectonic situation of the Bismarck Archipelago, after Herzig *et al.* (1994).

of Irvine (1982), the xenolith is a clin amphibole mesocumulate with the following mineralogical composition: 90% clin amphibole, 5% silicate glass, 2% clin oatacamite, 1% apatite, 1% sulfide, 1% vesicles, traces of biotite and magnetite.

The olive-green, mostly euhedral prisms of clin amphibole reach a length of more than 20 mm and display a microscopically visible zoning (*cf.* Fig. 2). In addition to a faintly brownish rim due to increasing Ti content, irregularly formed resorption features are present in the core of the crystals. In rare cases, the amphibole includes magmatic biotite and magnetite. Apatite is the only mineral phase that formed by direct crystallization of the silicate melt in the pockets between the amphibole crystals. Apatite crystals are mainly euhedral and reach a length of about 2 mm.

The intercumulus melt displays distinct exsolution-induced features: 1) exsolution of a Cu-Fe sulfide melt, 2) exsolution of a Cu-salt-hydrate melt, 3) exsolution of a second silicate melt, and 4) exsolution of a vapor phase.

Figure 2 shows the droplet-like external shape of the Cu-Fe sulfides. During the settling of the crystals that form the cumulate, a distinct deformation of these melt

droplets by the amphibole crystals took place. The small (0.1 mm) dark globules visible in Figure 3 represent a second, immiscible silicate melt in the sense of Philpotts (1982). Greenish blue polycrystalline monomineralic aggregates of clin oatacamite also are present (Figs. 2-4). The external shape of these aggregates is round or globular; they contain crystals of very variable sizes and habits (Fig. 4). Figure 5 testifies to the formation of the clin oatacamite as an exsolution from the silicate melt, as it shows the arrested process of the contemporaneous crystallization of apatite from the silicate melt and the exsolution of Cu-salt hydrate melt "frozen" by the submarine eruption of the host lava. Small drops of clin oatacamite hinder the growth of a euhedral crystal of apatite. These drops could well have formed melt inclusions if the apatite had had the chance to grow further. The distribution of vesicles holding the gas phase (Figs. 2, 3) is rather homogeneous within the intercumulus silicate melt, although accumulations occur in some places.

There is no indication of late hydrothermal alteration or weathering (*e.g.*, devitrification, formation of spherulites, perlitic cracks or the occurrence of secondary clay minerals) of the silicate glasses.

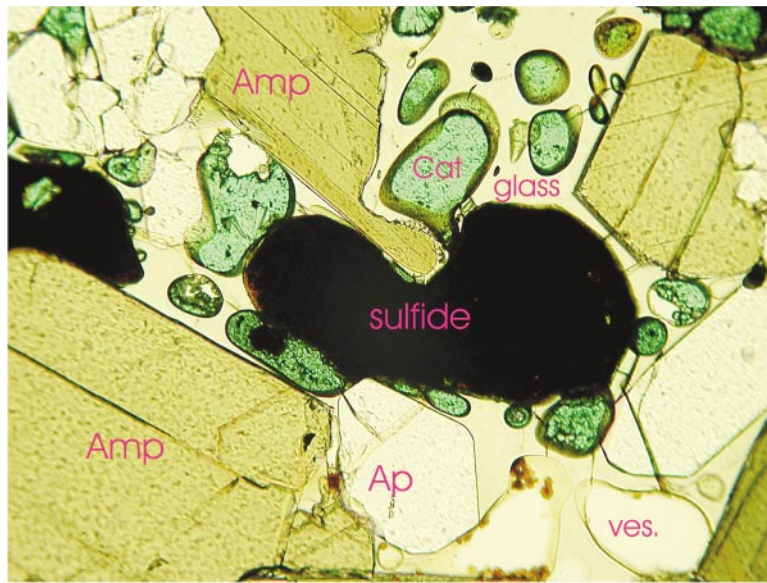


FIG. 2. Deformation of the exsolved sulfide and Cu-chloride salt-hydrate melts (Cat), due to the movement of amphibole (Amp) crystals in the silicate melt. Some amphibole crystals are corroded by the silicate melt. The melt is enriched in newly formed euhedral crystals of hydroxylapatite (Ap). Parallel polars; width of the field of view: 5 mm.

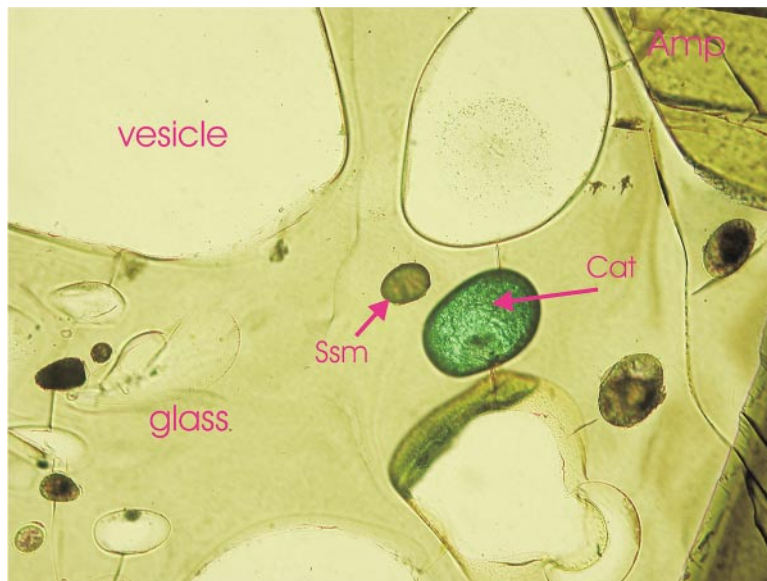


FIG. 3. Vesicular glass with signs of exsolution of an immiscible second silicate melt (Ssm) and a green Cu-salt-hydrate melt (Cat) in glass. Parallel polars; width of the field of view: 5 mm.

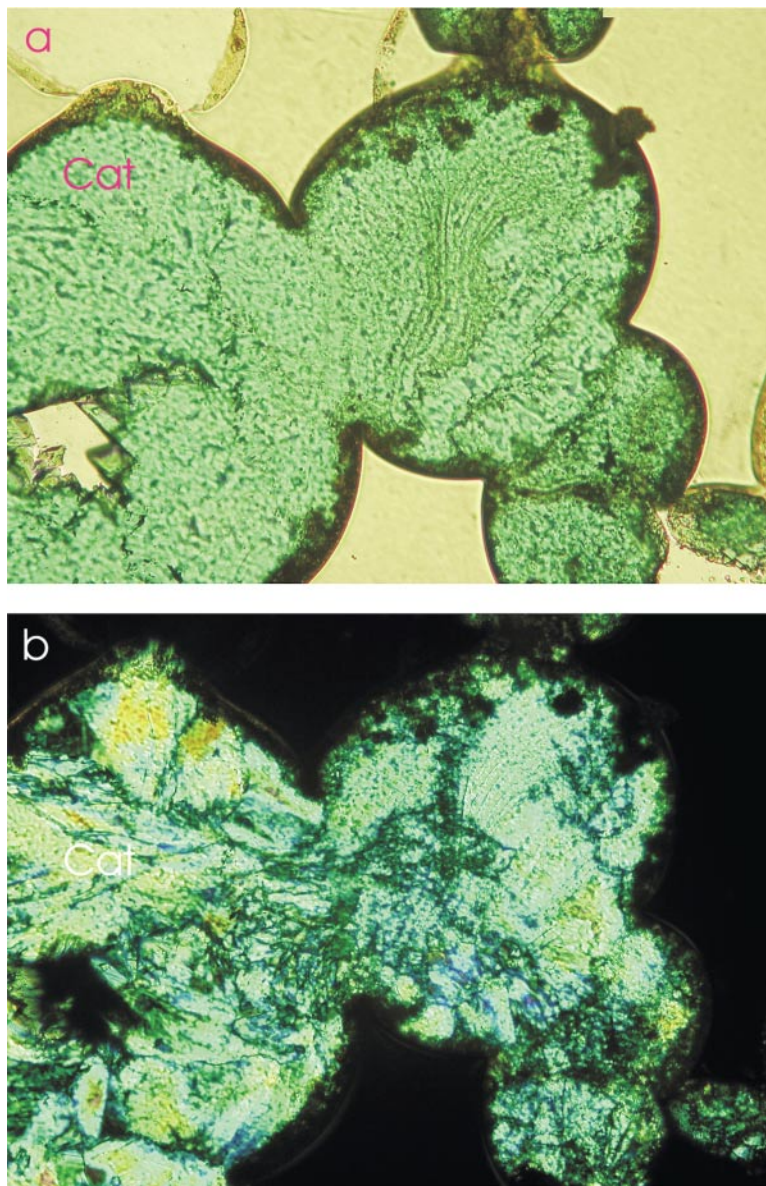


FIG. 4. Clinoatacamite (Cat) showing a droplet-like external form with internal aggregates of anhedral crystals of very variable sizes and shapes, (a) with parallel polars, and (b) with crossed polars; width of the field of view: 4 mm.

MINERALOGY AND COMPOSITION
OF THE CRYSTALLINE PHASES IN THE XENOLITH
AND THE HOST TRACHYBASALT

Amphibole

The clin amphibole of the cumulate is classified as magnesiohastingsite following the IMA nomenclature (Leake *et al.* 1997). The crystals have an elevated concentrations of K (about 1.7 wt.% K₂O) and show irregular patterns of zonation (*cf.* Table 1). Fluorine and chlorine contents are below the detection limit of the electron microprobe.

The clin amphibole in the host trachybasalt shows distinct optical and compositional zoning from a dark brown, Al-rich pargasitic core to an olive green, magnesiohastingsitic rim. Remarkably, the composition

TABLE 1. SELECTED COMPOSITIONS OF CALCIC AMPHIBOLE FROM THE MAGNESIOHASTINGSITE-DOMINANT CUMULATE, TUBAF SEAMOUNT, PAPUA NEW GUINEA

	F1-1 Mht	F1-13 Mht	F3-1 Prg	F1-13 Prg
SiO ₂ wt.%	39.71	38.82	40.05	40.03
TiO ₂	1.08	1.09	1.11	1.15
Al ₂ O ₃	13.19	13.86	13.82	13.72
Fe ₂ O ₃	4.36	4.13	3.52	2.97
Cr ₂ O ₃	0.03	0.04	0	0.03
MgO	13.92	12.67	12.97	12.99
CaO	11.99	11.74	11.92	11.78
MnO	0.18	0.20	0.21	0.21
FeO	7.97	9.79	10.02	10.38
Na ₂ O	2.25	2.35	2.24	2.31
K ₂ O	1.71	1.75	1.67	1.71
Total	97.29	96.45	97.52	96.38

Symbols: Mht: magnesiohastingsite, Prg: pargasite. Electron-microprobe data, specimen 54-2P.

TABLE 2. COMPOSITION OF MICA FORMED AS A MAGMATIC INCLUSION IN THE AMPHIBOLE CRYSTALS OF THE MAGNESIOHASTINGSITE-DOMINANT CUMULATE, TUBAF SEAMOUNT, PAPUA NEW GUINEA

SiO ₂ wt.%	Si <i>apfu</i>	2.749	Ba-Bt	0.14
TiO ₂	^{IV} Al	1.251	Ti-Bt	7.28
Al ₂ O ₃	ΣT	4.000	Tlc-Min	8.08
Cr ₂ O ₃	^{VI} Al	0.171	Eas-Sid	17.12
MgO	Cr	0.002	Won	9.53
CaO	Ti	0.073	Phl-Ann	57.85
MnO	Fe ²⁺	0.741		
FeO	Mn	0.008	Total	100.00
BaO	Mg	2.008	X _{Mg}	0.73
Na ₂ O	ΣO	3.003		
K ₂ O	Ba	0.001		
H ₂ O	Ca	0.005		
F ⁻	Na	0.095		
Cl ⁻	K	0.816		
	ΣI	0.918		
Total	OH	1.998		
	F	0.001		

The composition is the average result of 56 electron-microprobe analyses of specimen 54-2P. The structural formula is calculated on the basis of 12 atoms of oxygen per formula unit (*apfu*). The mica is classified as phlogopite.

of the rim of these crystals strongly resembles the clin amphibole in the cumulate (Table 1).

Phlogopite

Phlogopite flakes, which occur as magmatic inclusions in magnesiohastingsite of the cumulate, yield X_{Mg} values in the range 0.71–0.75 and TiO₂ contents of 1.25–1.45 wt.%. Slight variations in composition are recorded from grain to grain. As in the magnesiohastingsite, the F and Cl contents are very low (<0.01 wt.%).

Phlogopite in the trachybasaltic host-rock has higher X_{Mg} values (about 0.85) and lower TiO₂ contents (0.9–1.0 wt.%) than the phlogopite in the cumulate, but the F and Cl contents are similarly low. Representative compositions of phlogopite are presented in Table 2.

Plagioclase

Relatively large (0.3–0.5 mm) phenocrysts of plagioclase as well as tiny crystals in the matrix of the trachybasalt show normal zoning, with An_{38–48} in the core and An_{25–28} at their rim, whereas feldspar is absent in the cumulate xenolith.

Magnetite

Magnetite inclusions in amphibole of the cumulate contain about 3.8 wt.% TiO₂ and elevated concentrations of Al (4.3–4.5 wt.% Al₂O₃; *cf.* Table 3).

Octahedra in the matrix of the host rock have distinctly higher Ti contents, up to 12.7 wt.% TiO₂ and slightly lower concentrations of Al (2.6–2.9 wt.% Al₂O₃; *cf.* Table 3). As in the magnetite of the cumulate, zoning is not present.

TABLE 3. REPRESENTATIVE COMPOSITIONS OF THE MAGNETITE FORMED AS MAGMATIC INCLUSIONS IN THE MAGNESIOHASTINGSITE-DOMINANT CUMULATE, TUBAF SEAMOUNT, PAPUA NEW GUINEA

	F5-4	F5-5	F5-7		F5-4	F5-5	F5-7
SiO ₂ wt.%	0.09	0.08	0.09	Mg <i>apfu</i>	0.111	0.105	0.106
TiO ₂	3.72	3.66	3.8	Ca	0.002	0.001	0.001
Al ₂ O ₃	4.47	4.37	4.32	Mn	0.013	0.012	0.012
Cr ₂ O ₃	0.04	0.02	0.02	Fe ²⁺	0.877	0.884	0.884
Fe ₂ O ₃	58.15	57.93	57.47	ΣA	1.003	1.003	1.003
MgO	2.04	1.91	1.93				
CaO	0.06	0.04	0.03	Si	0.003	0.003	0.003
MnO	0.41	0.40	0.38	Ti	0.102	0.101	0.105
FeO	32.1	32.08	32.08	Al	0.192	0.189	0.188
				Cr	0.001	0	0.001
Total	101.07	100.49	100.11	Fe ³⁺	1.596	1.602	1.595
				Fe ²⁺	0.102	0.101	0.105
				ΣB	1.997	1.997	1.997

The structural formula (AB₂O₄) is based on three cations and four atoms of oxygen per formula unit; A + B = 3 *apfu*. The proportion of Fe²⁺ and Fe³⁺ is thus fixed by stoichiometry. Specimen 54-2P, results of electron-microprobe analyses.

Apatite

Euhedral crystals of hydroxylapatite in the melt pockets of the cumulate contain low contents of Cl (0.05–0.09 wt.%) and elevated contents of F, ranging between 0.82 and 1.26 wt.%. The levels of the rare-earth elements and Ba are below the detection limit of the electron microprobe (*cf.* Table 4).

GEOCHEMICAL AND MINERALOGICAL FEATURES OF THE INTRACUMULATE SILICATE GLASS AND THE EXSOLVED MELT PHASES OF THE XENOLITH

Silicate glass

Electron-microprobe investigations of the intercumulus silicate glass reveal its homogeneity except for phosphorus (which shows a significant enrichment over a distance up to 100 μm toward the newly formed hydroxylapatite) and titanium (which is enriched over a similar distance near the amphibole crystals). In Table 5, we summarize the mean values and the standard deviations obtained from 98 analyses of the glass and, for comparison, the composition of the trachybasaltic host-rock. Distribution histograms for the SiO_2 , K_2O , P_2O_5 and Cl concentrations in the glass are presented in Figures 6a–d. With the help of boxplots (Figs. 7a, b), it is possible to show how the composition of the glass changes in different pockets of melt. The amount of Na remains stable in all pockets investigated, whereas the level of P changes from pocket to pocket and shows a broader range within the same pocket, depending on the amount of apatite present.

Figure 8 is a projection of the analytical results in terms of the total alkalis *versus* silica (TAS) diagram

(Le Maitre 2002). The compositions of the intercumulus glass, which correspond to trachyandesite or tephriphonolite, have a completely different composition than the trachybasaltic host-rock.

Exsolved silicate melt

Owing to the very small volume of the exsolved second silicate melt, it was only possible to measure the chemical composition of two exsolved areas. The glass is silica-undersaturated, enriched in Fe, Mg, Ca and Ti, and shows lower concentrations of Na, K and Al (*cf.* Table 5). According to the TAS classification, it is a foiditic glass.

TABLE 4. COMPOSITION OF THE MOST FLUORINE-RICH AND FLUORINE-POOR APATITE FORMED AS A SINGLE MINERAL BY CRYSTALLIZATION FROM THE LATE-STAGE MELT IN MELT POCKETS BETWEEN THE AMPHIBOLE CRYSTALS, SIMULTANEOUSLY WITH THE EXSOLUTION OF THE IMMISCIBLE MELTS, TUBAF SEAMOUNT, PAPUA NEW GUINEA

	F1-1	F3-18		F1-1	F3-18
SiO ₂ wt.%	0.56	0.30	Si <i>apfu</i>	0.048	0.026
P ₂ O ₅	40.11	40.58	P	2.880	2.934
SrO	0.41	0.44	Sr	0.020	0.022
CaO	56.71	55.28	Ca	5.153	5.060
MnO	0.06	0.08	Mn	0.004	0.006
FeO	0.22	0.20	Fe	0.016	0.014
Na ₂ O	0.16	0.14	Na	0.027	0.023
H ₂ O	1.37	1.14	Σ cations	7.861	7.861
F	0.82	1.26			
Cl ⁻	0.05	0.08	OH	0.774	0.648
			F	0.219	0.341
Total	100.46	99.50	Cl	0.007	0.011

The structural formula is calculated on the basis of 13 atoms of oxygen per formula unit. Specimen 54-2P, electron-microprobe data. Both compositions correspond to hydroxylapatite.

TABLE 5. MEAN ANALYTICAL VALUES AND OTHER STATISTICAL DATA PERTAINING TO THE SILICATE GLASS IN THE MAGNESIOHASTINGSITE-DOMINANT CUMULATE, COMPARED WITH THE COMPOSITION OF THE IMMISCIBLE SILICATE LIQUID AND THE TRACHYBASALTIC HOST-ROCK OF THE XENOLITH, TUBAF SEAMOUNT, PAPUA NEW GUINEA

	SiO ₂	TiO ₂	Al ₂ O ₃	Cr ₂ O ₃	Fe ₂ O ₃	FeO	MgO	MnO	CaO	BaO	Na ₂ O	K ₂ O	P ₂ O ₅	Cl	S	Total
<i>n</i>	98	98	98	98	98	98	98	98	98	98	98	98	98	98	21	98
Mean	54.14	0.36	19.01	0.02	n.d.	4.87	2.02	0.15	5.61	0.01	5.58	4.02	0.17	0.14	0.037	96.07
Median	54.12	0.36	19.02	0.01	n.d.	4.87	2.05	0.15	5.63	0.02	5.59	4.02	0.13	0.14	0.036	96.17
S.D.	0.64	0.06	0.28	0.02	n.d.	0.37	0.28	0.03	0.28	0.02	0.33	0.16	0.11	0.02	0.009	0.58
Range	3.19	0.27	1.39	0.08	n.d.	1.54	1.29	0.18	1.41	0.08	3.21	0.82	0.41	0.09	0.04	3.68
Minimum	52.53	0.23	18.38	0.00	n.d.	4.04	1.30	0.06	4.71	0.00	2.85	3.71	0.03	0.10	0.014	93.37
Maximum	55.73	0.50	19.77	0.08	n.d.	5.58	2.59	0.24	6.11	0.08	6.05	4.54	0.43	0.19	0.055	97.05
Second																
sil. liquid	41.03	1.05	13.23	0.10	n.d.	13.08	13.72	0.16	11.76	0.00	2.26	1.70	0.00	0.01	n.d.	98.04
Host rock	46.20	0.77	15.00	0.02	5.73	3.93	7.47	0.22	9.84	n.d.	3.78	2.15	0.84	n.d.	n.d.	97.5

Compositions are reported in wt.%. The number of electron-microprobe analyses (*n*) is 98 in the case of the silicate glass, but equal to 2 in the case of the immiscible silicate liquid. n.d.: not determined.

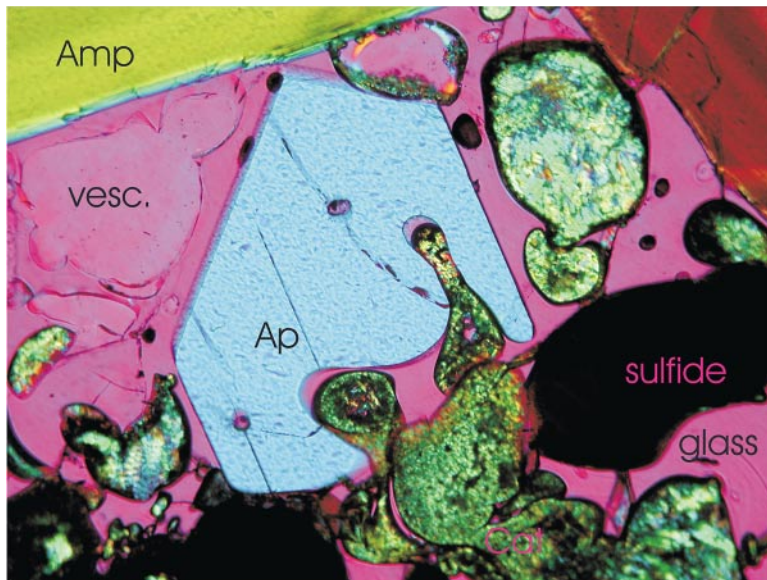


FIG. 5. Intergrowth of a newly formed crystal of hydroxylapatite (Ap) with exsolved Cu-salt-hydrate melt (Cat). Apatite shows crystal faces in contact to the silicate melt and vesicles, whereas re-entrant interfaces and melts inclusions are formed in contact with Cu-salt-hydrate melts. Crossed polars + compensator (λ 650 nm). Width of field of view: 1 mm.

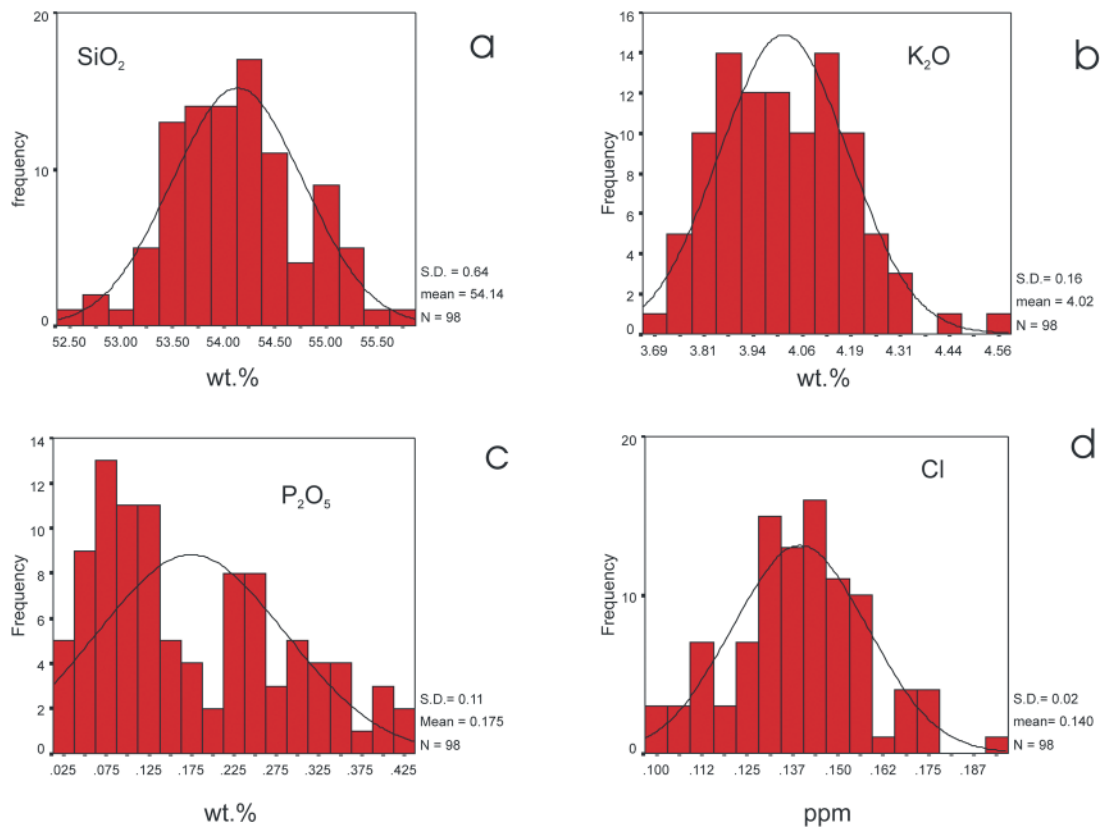


FIG. 6. Histograms of the concentrations of (a) SiO₂, (b) K₂O, (c) P₂O₅ and (d) Cl in the silicate glass. Results of 98 microprobe analyses are shown. The distribution of SiO₂, K₂O, and Cl is homogeneous, whereas P₂O₅ shows a broad distribution due to the different amount of apatite in the melt pockets.

Sulfide melt

Figure 9 is a back-scattered electron image of the Cu-Fe sulfide minerals, which crystallized from globules of sulfide melt. The crystals exhibit very small exsolution-induced features not broader than 3 μm , rendering the analysis of the exsolved phase impossible. Analyses of spots with diameters of $25 \times 25 \mu\text{m}$ revealed only the presence of Fe, Cu and S; other chalcophile elements are below the detection limit of the electron microprobe. These analyses indicate compositions that range between chalcopyrite and intermediate solid-solution (*Iss*). X-ray-diffraction analyses of single droplets of sulfide indicate the presence of cubanite and smaller amounts of chalcopyrite. Owing to the complex character of the XRD patterns, we still

do not know if isocubanite (Caye *et al.* 1988) is present in the sample.

Salt-hydrate melt

On the basis of their shape, we interpret the domains of Cu-salt-hydrate melt as due to exsolution from the intercumulus melt. Electron-microprobe investigations of the domains of Cu-salt hydrate show a very constant composition, with a mean of 61.45% Cu, 16.8% Cl and 21.17% O + H, whereas the Zn content is near the detection limit of the electron microprobe ($<0.01\%$). The theoretical composition of $\text{Cu}_2(\text{OH})_3\text{Cl}$ is 59.51% Cu, 22.47% O, 16.6% Cl, and 1.42% H. Figure 10 shows an electron-microprobe profile of one domain of Cu-salt-hydrate melt.

An X-ray-diffraction analysis on small samples proved that only clinoptacumite is present. An FTIR spectroscopic investigation of single crystals and of pressed powder tablets shows, by comparison with the data of Moenke (1966) and Sharkey & Lewin (1972), that no other anion complex (*e.g.*, CO_3^{2-} , SO_4^{2-} or PO_4^{3-}) is present in the samples.

GEOCHRONOLOGY

For the $^{40}\text{Ar}/^{39}\text{Ar}$ age determination, a plateau could be calculated for increments 3–7, with 99.9% of the

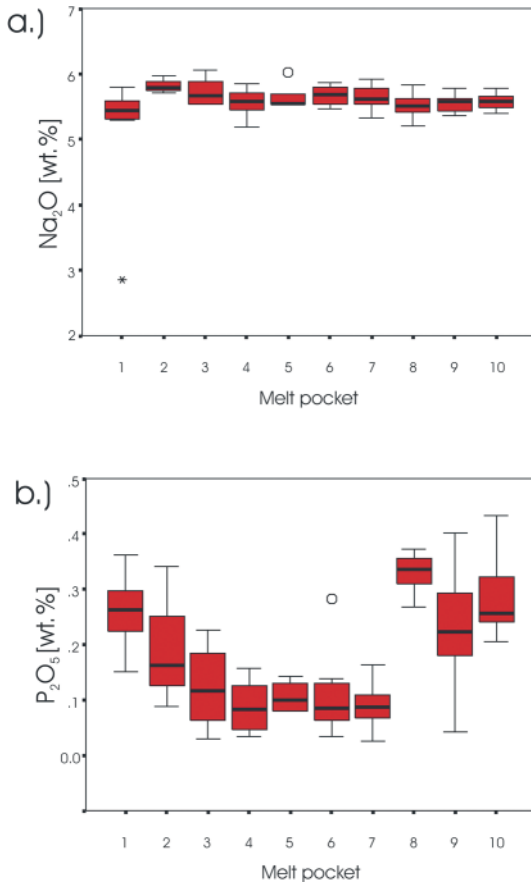


FIG. 7. Boxplots of the (a) Na_2O and (b) P_2O_5 contents in ten different pockets of melt. The Na_2O remains stable in all pockets, but the P_2O_5 changes from pocket to pocket and shows a greater range in the domains of glass. The inhomogeneous behavior of phosphorus depends on the different amount of apatite in the areas of melt.

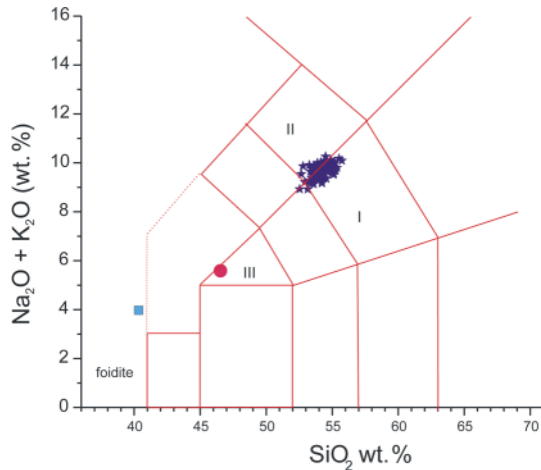


FIG. 8. Projection of the results of electron-microprobe analyses of the silicate glass and of the immiscible silicate liquid, and the composition of the host rock in the TAS diagram (Le Maitre 2002). The glass compositions are classified as trachyandesite (I), tephriphonolite (II) and foidite, and the host rock as a trachybasalt (III). Symbols: star: intracumulate glass, square: immiscible silicate liquid, circle: host rock.

observed ^{39}Ar almost completely determined by increment 6 (1400 K). This plateau represents an age of 0.51 ± 0.96 Ma. Several isochrons can be calculated; the one with the best fit represents increments 4, 6, and 7 and gives an age of 0.21 ± 0.08 Ma. The other isochrons give ages similar to the plateau ages. All isochron and plateau ages overlap at one sigma. This finding is the consequence of the large errors in the analysis, owing to the very young age and the low K-content of the magnesiohastingsite compared to the micas usually used. These ages are in accordance with the K–Ar ages on biotite of a monzonite and volcanic rocks from the nearby Lihir Island, which yielded 0.917 ± 0.1 Ma and 0.342 ± 0.036 Ma, respectively (Moyle *et al.* 1990), and the age of the mineralization on Lihir Island (Davies & Ballantyne 1987).

DISCUSSION

The petrographic, mineralogical and geochemical results show clearly that both the clinoatacamite and the Cu–Fe sulfide formed by exsolution as immiscible melts from the intercumulus silicate melt. It seems absolutely clear that clinoatacamite was not generated by hydrothermal alteration or submarine weathering. In its high-temperature formation by unmixing, it differs clearly from all known descriptions.

Compared to pure Cu^{2+} halides, hydroxychlorides are much more stable in nature. The three polymorphic minerals with the formula $\text{Cu}_2(\text{OH})_3\text{Cl}$ are atacamite (Parise & Hyde 1986), botallackite (Hawthorne 1985, Hawthorne & Groat 1985) and clinoatacamite (Grice *et al.* 1996). Although the mineral paratacamite (Fleet 1995) yields a similar composition, it is not considered

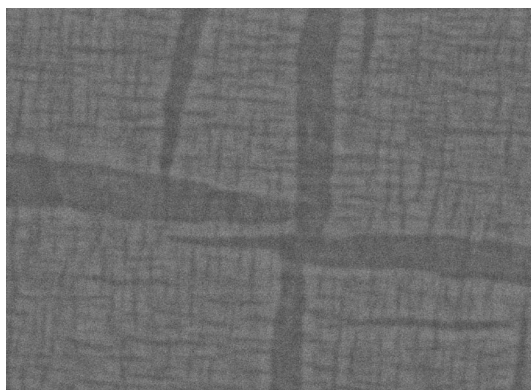


FIG. 9. Back-scattered electron image of the exsolution features in the crystallized of Cu–Fe sulfide melt. The bright areas represent the cubanite, and the darker ones, the chalcocopyrite. Width of the field of view: $37.5 \mu\text{m}$.

to be a true polymorph of $\text{Cu}_2(\text{OH})_3\text{Cl}$ [*cf.* Grice *et al.* (1996), Jambor *et al.* (1996) for discussion]. Paratacamite contains considerable amounts of Zn and was re-defined as $\text{Cu}_3(\text{Cu}_{1-x}\text{Zn}_x)(\text{OH})_6\text{Cl}_2$ ($x > 0.5$). Therefore, numerous early descriptions of paratacamite have had to be changed to clinoatacamite, especially in the case of synthetically produced Zn-free phases.

Botallackite, the metastable of the three natural polymorphic $\text{Cu}_2(\text{OH})_3\text{Cl}$ compounds, generally precipitates from aqueous solutions and later transforms to atacamite or clinoatacamite (Pollard *et al.* 1989, Hannington 1993).

Atacamite occurs commonly in the oxidation zone of primary deposits of copper, where it is of local importance as ore mineral. Furthermore, atacamite may be a constituent of submarine, metalliferous muds and form part of the oxidized portions of black smoker deposits in association with the other secondary minerals of Cu (Hannington 1993, Damyanov *et al.* 1998, Mills *et al.* 1996, Butozova *et al.* 1989). Atacamite also may form by exhalation processes, as observed in fumaroles of the Vesuvius – Monte Somma system (Ragone & Ottone 1997) or in Kamchatka (Serafimova *et al.* 1994).

Clinoatacamite may form in the hydrothermal and diagenetic environment, but also as exhalations at burning coal dumps (Witzke 1996) and in fumaroles of various volcanos like the Nyamuragira in the Democratic Republic of Congo, the Cerro Negro in Nicaragua (Stoiber & Rose 1973) and volcanos in Kamchatka (Serafimova *et al.* 1994).

Several experiments and theoretical calculations of the stability of the different Cu–Cl phases have focused on the acquisition of thermochemical data in aqueous fluids in the temperature range between 0° and 100°C . This activity was triggered by a general interest in the geochemistry of the oxidation zone of ore deposits and corrosion prevention. Two groups extended the experiments to higher temperatures. Babčan & Ševc (1973) investigated the stability of secondary copper minerals in the system $\text{Cu}^{2+} - \text{HCO}_3^- - \text{Cl} - \text{CO}_3^{2-} - \text{H}_2\text{O}$, and found atacamite to be stable up to 200°C at low values of pH. Sharkey & Lewin (1971, 1972) showed the stability of paratacamite (which certainly should be revised as clinoatacamite) up to temperatures of 500°C . During heating, all other polymorphs are spontaneously converted to clinoatacamite. All these investigations on the stability of $\text{Cu}_2(\text{OH})_3\text{Cl}$ polymorphs were performed at low pressures.

Direct evidence for the transport of copper as a Cu–chlorine phase in magmatic systems is rare (*e.g.*, Lowenstern *et al.* 1991, Lowenstern 1993, 1994). Yang & Scott (1996) detected copper-bearing fluids in andesites from the PACMANUS polymetallic sulfide deposit (Manus basin, western Pacific). Campos *et al.* (2001) described the occurrence of Cu chlorides in melt inclusions in the Llamo porphyry unit of the Zaldívar Cu-deposit, in northern Chile. For metalliferous brines of the Cheleken Peninsula, Lebedev (1983) postulated the

transport of copper as a complex. All authors refer to the close connection between the sulfide-bearing and the chloride-bearing systems.

The stability of cuprous halides in technical glasses, mainly borosilicate glasses, up to 1450°C (Araujo 1998) leaves room for interesting speculations about the role of such phases in natural melts and glasses.

There are different possibilities to consider to explain the formation of the xenolith studied. It could have formed 1) as a true xenolith from a clinooctamite-bearing altered part of the seafloor, which was reincorporated and remelted by the host trachybasaltic melt, 2) as a completely solidified cumulate, which was intruded by the ascending trachybasaltic melt, 3) as a clinooamphibole xenolith that experienced partial melting due to rapid heating and decompression during ascent, or 4) as an independently developed cumulate whose formation was stopped by the intrusion of the trachybasaltic magma into its magma chamber. The textures described were frozen during the quick ascent and subsequent eruption at the seafloor.

We can rule out the first hypothesis. A reheated and remelted part of the altered ocean floor should show completely different petrographic features, like relict cores in the magnesiohastingsite, and relict minerals in the glass, like epidote or plagioclase. We found no other sample in the extensive collection of xenoliths from TUBAF Seamount that could support such an assumption.

The results of X-ray-fluorescence and electron-microprobe analyses clearly show that the composition of the host rock and of the intercumulus silicate glass is completely different. Therefore, formation by infiltration from the host magma can be excluded. The influence of a more fractionated melt of the trachybasaltic volcanic system seems improbable. It is impossible to model the composition of the intercumulus melt by fractional crystallization of magnesiohastingsite (\pm apatite) from the host trachybasalt. The formation of a second cumulate with a different mineralogical composition is possible but considered very unlikely. For this reason, we not consider the second hypothesis likely.

The genesis of a partial melt in a magnesiohastingsite cumulate by a rapid heating and decompression of the xenolith in the sense of Schiano *et al.* (1995) can be excluded owing to the lack of textural proof for dehydration-induced melting of the amphibole. Furthermore, a melt generated by the sole breakdown of magnesiohastingsite should have a lower K-content and should bear some restitic phases. More important is the fact that we found no signs of the formation of melt in the more fertile xenoliths from the TUBAF Seamount (*e.g.*, gabros). Furthermore, Franz *et al.* (2002) found no evidence for the reheating of ultramafic xenoliths by the trachybasaltic host-rock.

We consider the fourth hypothesis the most probable one. We postulate an independent formation of the cumulate and its intercumulus melt in a magma cham-

ber underneath the TUBAF Seamount. We are aware of the fact that the possible role of diffusion processes could be underestimated. It is not unusual that such isolated melts change their composition far away from the original magma (*cf.* Philpotts 1990, p. 250-251), and this possibility seems to apply to our sample. Temperatures of crystallization of the cumulate can be estimated with the geothermometer of Righter & Carmichael (1996), which is based on exchange of Ti between melt and phlogopite phenocrysts. Assuming equilibrium between phlogopite in the cumulate and the intercumulus melt, temperatures of $1039^\circ \pm 50^\circ\text{C}$ can be calculated using the average composition of trachyandesitic melt and the phlogopite.

We do not know why there was such a predominant "refinement" of Cu and Fe in the silicate melt.

The unmixing of the sulfide melt

The basic requirement for the unmixing process is the saturation of the silicate melt in a Cu-Fe-S liquid. According to investigations of Wallace & Carmichael (1992), sulfur concentrations in hyaline submarine lavas are much higher than in subaerial lavas. The sulfur content of pre-eruptive basalts ranges between 800 and 2500 ppm. In these magmas, signs of the unmixing of sulfide melt are quite common, as indicated by the presence of sulfide globules in glassy rims of pillows (*e.g.*, Czamanske & Moore 1977). Such exsolved melts, however, are usually Fe-S-O liquids, so that on cooling an association of pyrrhotite or pentlandite with small amounts of magnetite crystallizes (Doyle & Naldrett 1987). In contrast, the melts in the cumulate from TUBAF Seamount are Cu-Fe-S liquids. To our knowledge, no experimental results are available to give saturation data of such a melt component in silicate melts. Electron-microprobe analyses of the intercumulus silicate melts of sample 54-2P reveal sulfur contents of 140-550 ppm, giving an indication of the concentration of sulfur in tephriphonolitic melts needed to achieve saturation in a sulfide melt. Mineralogical and geochemical data indicate that the unmixing of that melt must have taken place in a temperature range between 960° and 557°C. The first temperature is the upper stability limit of *Iss* (Craig & Scott 1974), and the lower estimate refers to chalcopyrite appearing as a stable phase (Cabri & Hall 1972, Cabri 1973).

The unmixing of the Cu-salt-hydrate melt

Information about the saturation of silicate melts with various chlorine species is supplied by Webster (1997) and Signorelli & Carroll (2000). However, data on the solubility in Cu-Cl-silicate melt systems are missing. As a result, the NaCl-silicate melt systems of Carroll & Webster (1994, see also Lowenstern 2000) must be used for reference. The data on these systems show that unmixing of a chlorine-bearing melt from a

silicate melt is a very complex process. Anhydrous and H₂O-poor silicate melts saturated in chlorine unmix simple *Me*-Cl salt melts. In H₂O-rich silicate melts, which coexist with a vapor phase, chlorine is preferably enriched in the H₂O-dominant vapor. With rising concentrations of Cl, the system becomes non-ideal, and the Cl content in the volatile phase increases distinctly more quickly than in the melt (Carroll & Webster 1994). At temperatures typical of magmatic systems, the binary system NaCl-H₂O and also the system silicate melt - NaCl - H₂O are distinguished by a miscibility gap. In the latter case, unmixing creates a salt-hydrate melt coexisting with a silicate melt and a vapor phase. Any changes in the concentration of Cl only result in changes of the relative proportions of the phases, but do not lead to changes in the concentration of Cl in the phases (Sourirajan & Kennedy 1962, Lowenstern 2000).

The concentration of Cl in a buffered silicate melt strongly depends on the melt's composition, especially its [Mg + Na + Fe + Al] / Si value, whereas the influence of temperature and pressure is relatively weak (*cf.* Webster 1997). Metrich & Rutherford (1992) observed Cl concentrations of about 2700 ppm in rhyolites, and even somewhat elevated concentrations of Cl in andesites and basalts. Mixed-volatile systems of CO₂ and Cl phases entail the phase separation of the Cl-bearing species at a lower vapor-pressure. According to Joyce & Holloway (1993), the presence of CO₂ permits unmixing of salt-hydrate melts up to pressures of 500 MPa. These

experiments show that the whole oceanic crust from the crust-mantle interface to the ocean floor can bear silicate melts in coexistence with vapor and salt-hydrate melts. Although these experiments are only based on silicate melt - NaCl - H₂O systems, a transfer to more complex Cu - Fe - S - Cl - H₂O - CO₂(?) - silicate melt seems to be justified. Candela & Piccoli (1995, see also Kamenetsky *et al.* 2002), for instance, demonstrated that the presence of CO₂ increases the process of metal fractionation in ore-bearing magmatic systems.

CONCLUSIONS

The observation of a Cu-Cl-salt-hydrate melt and a Cu-sulfide melt in equilibrium with two mafic silicate melts within a magnesiohastingsite cumulate xenolith puts new constraints on processes of segregation and transport of ore-forming agents. In Table 6, we present the sequence of petrological events leading to this unique assemblage of former melt phases. The intrusion of a mafic magma at the base of the oceanic crust and its subsequent cooling led to the crystallization of the magnesiohastingsite cumulate and the formation of its intercumulus melt.

The strong "refinement" of Cu, Fe, S and Cl in the intercumulus silicate melt is not yet fully understood. Experimental investigations on technical borosilicate melts (Araujo 1998) show that cuprous halides form separate phases up to temperatures of 1450°C. Whether

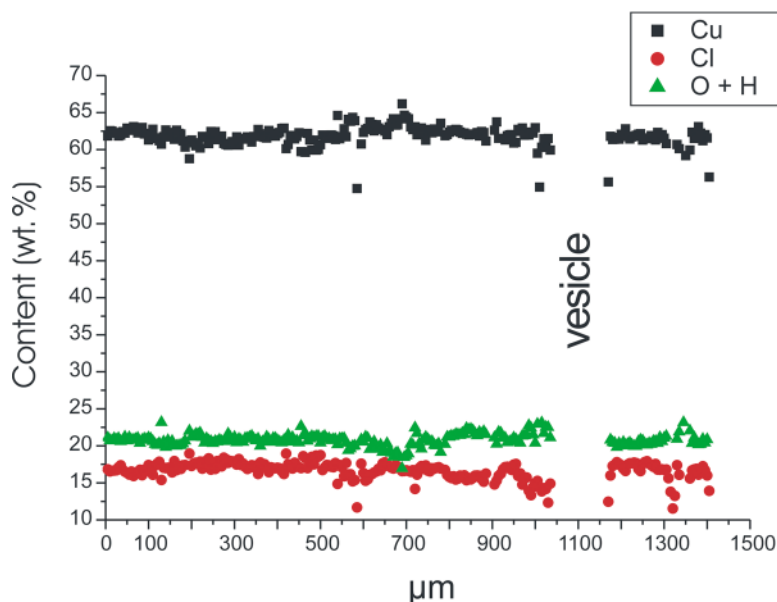


FIG. 10. Microprobe profile (281 analyses with a 5-µm step width of the analytical points) along a droplet of exsolved Cu-salt-hydrate melt showing the homogeneity of the clinotacumite. The sum (O + H) was calculated as the difference from 100%.

the enrichment of these phases took place by diffusion, coagulation or another process is not known. Although the existence of such separate Cu-phases in natural melts has not been observed or postulated, one can assume that they may be important during high-temperature fractionation in mafic melt-dominated systems.

Further cooling in the magma chamber led to the crystallization of hydroxylapatite and triggered liquid immiscibility in the intercumulus melt. The formation of the Cu–Fe–S melt took place in a temperature range between 960° and 557°C, whereas experiments point to an upper-temperature limit of 800°C for the unmixing of the salt-hydrate melt. Contemporaneously, the unmixing of a volatile (probably CO₂-bearing) fluid phase took place.

Decreasing temperatures brought about the crystallization of clinoatacamite and of *Iss*, the latter exsolving to cubanite and chalcopyrite below 557°C. At this stage, a new pulse of trachybasaltic magma, injected into the magma chamber, disrupted the cumulate and transported part of it as xenoliths to the seafloor, where the unmixing textures were frozen. The young age of the TUBAF Seamount prevented the long-term influence of seawater and, consequently, an annealing of the features described.

The observation of these unmixing processes sheds new light on the *modus operandi* of how metal-enriched magmatic fluids enter hydrothermal systems. If, for example, a fluid phase penetrated a deep-seated cumulate enriched in Cu–Cl and Cu sulfide compounds, an immediate mobilization of these elements would occur. This possibility may have important implications for the formation of epithermal gold deposits such as the giant Ladolam mine on nearby Lihir Island or Conical Seamount (Müller *et al.* 2003), a possible submarine ana-

log of Ladolam, located in the immediate vicinity of Lihir and TUBAF Seamount.

ACKNOWLEDGEMENTS

The authors thank the master, officers and crew of research vessel R/V Sonne for the logistical support and good cooperation during our research activities in the New Ireland basin. Thanks are also due to Klaus-Peter Becker and Ulf Kempe (both of Freiberg) for help with the geochemistry and the electron-microprobe analyses. Wolfgang Voigt (Institut für Anorganische Chemie Freiberg) and Matthias Müller (Otto-Schott-Institut für Glaschemie FSU, Jena) supported us with important information and inspiring discussions. We owe thanks to Dieter Dettmar (Bochum) for the preparation of the thin sections. Jacob B. Lowenstern and James E. Mungall are thanked for their in-depth reviews that greatly improved the manuscript. This work has benefited from the patient and encouraging editorial assistance of Robert F. Martin. Principal funding for this project was provided by the German Federal Ministry for Education and Research (BMBF Grant 03G0133A to Peter Herzig) and by the Leibniz Program of the German Research Foundation (DFG).

REFERENCES

- ARAÚJO, R. (1998): Influence of host glass on precipitation of cuprous halides. *J. Non-Cryst. Sol.* **223**, 53-56.
- BABČAN, J. & ŠEVČ, J. (1973): Beitrag zur Frage über die Entstehung und die Stabilität von Kupfermineralen im System Cu²⁺ – HCO₃⁻ – H₂O. *Geol. Zb. – Geol. Carp.* **XXIV** 1, 169-175.

TABLE 6. SEQUENCE OF PETROLOGICAL PROCESSES DURING THE FORMATION OF THE MAGNESIOHASTINGSITE-DOMINANT CUMULATE, TUBAF SEAMOUNT, PAPUA NEW GUINEA

1200°C	Intrusion of mafic magma and formation of a magma chamber Crystallization of the calcic amphibole cumulate and evolution of the intracumulate melt "Refinement" of the melt and its enrichment in Cu, Fe, S and Cl
960° – ~800°C	Crystallization of hydroxylapatite from the intracumulate melt Exsolution of the foiditic immiscible silicate melt Exsolution of a Cu–Fe–S liquid Exsolution of a Cu-salt-hydrate melt Formation of a vapor phase Crystallization of intermediate solid-solution (<i>Iss</i>) Crystallization of clinoatacamite
<557°C	Subsolvus crystallization of cubanite and chalcopyrite
2°C	Disruption of the cumulate by a pulse of trachybasaltic magma Transport of the xenolith of cumulate origin to the seafloor Freezing of the exsolved melt phases and the microstructures Formation of the TUBAF Seamount

- BARNES, H.L. (1979): Solubilities of ore minerals. In *Geochemistry of Hydrothermal Ore Deposits* (H.L. Barnes, ed.). John Wiley & Sons, New York, N.Y.
- BISCHOFF, J.L. & ROSENBAUER, R.J. (1987): Phase separation in seafloor geothermal systems: an experimental study of the effects on metal transport. *Am. J. Sci.* **287**, 953-978.
- BUTOZOVA, G.YU., SHTERENBERG, L.E., VORONIN, B.I. & GOR'KOVA, N.V. (1989): Atacamite in metal-containing sediments of the Atlantic Ocean. *Dokl. Akad. Nauk SSSR* **309**, 1177-1181 (in Russ.).
- CABRI, L.J. (1973): New data on phase relations in the Cu-Fe-S system. *Econ. Geol.* **68**, 443-454.
- _____ & HALL, S.R. (1972): Mooihoekite and haycockite, two new copper-iron sulfides, and their relationship to chalcopyrite and talnakhite. *Am. Mineral.* **57**, 689-708.
- CAMPOS, E., NIKOGOSIAN, I. & TOURET, J.R.L. (2001): Orthomagmatic copper origin in Zaldivar Cu-porphry deposit, Chile. *EUG XI, J. Conf. Abstr.* **6**, 787.
- CANDELA, P.A. & PICCOLI, P.M. (1995): Model ore-metal partitioning from melts into vapor-brine mixtures. In *Magma, Fluids and Ore Deposits* (J.F.H. Thompson, ed.). *Mineral. Assoc. Can., Short Course Vol.* **23**, 101-127.
- CARROLL, M.R. & WEBSTER, J.D. (1994): Solubilities of sulfur, noble gases, nitrogen, chlorine, and fluorine in magmas. In *Volatiles in Magmas* (M.R. Carroll & J.R. Holloway, eds.). *Rev. Mineral.* **30**, 231-279.
- CAYE, R., CERVELLE, B., CESBRON, F., OUDIN, E., PICOT, P. & PILLARD, F. (1988): Isocubanite, a new definition of the cubic polymorph of cubanite CuFe_2S_3 . *Mineral. Mag.* **52**, 509-514.
- COLEMAN, P.J. & KROENKE, L.W. (1981): Subduction without volcanism in the Solomon Island arc. *Geo-Marine Lett.* **1**, 129-134.
- CRAIG, J.R. & SCOTT, S.D. (1974): Sulfide phase equilibria. In *Sulfide Mineralogy* (P.H. Ribbe, ed.). *Rev. Mineral.* **1**, 1-110.
- CZAMANSKE, G.K. & MOORE, J.G. (1977): Composition and phase chemistry of sulfide globules in basalt from the Mid-Atlantic Ridge rift valley near 37°N lat. *Geol. Soc. Am., Bull.* **88**, 587-599.
- DAMYANOV, Z.K., DEKOV, V.M., LISITSYN, A.P., BOGDANOV, Y.A., AIDANLIISKI, G. & DIMOV, V.I. (1998): Mineralogical features of the near sulfide mound sediments. MIR zone, TAG hydrothermal field (Mid-Atlantic Ridge, 26°N). *Neues Jahrb. Mineral., Abh.* **174**, 43-78.
- DAVIES, R.M. & BALLANTYNE, G.H. (1987): Geology of the Ladolam gold deposit, Lihir Island, Papua New Guinea. *Proc. Pac. Rim Congress* **87**, 943-949.
- DOYLE, C.D. & NALDRETT, A.J. (1987): The oxygen content of "sulfide" magma and its effect on the partitioning of nickel between coexisting olivine and molten ores. *Econ. Geol.* **82**, 208-211.
- FLEET, M.E. & PAN, YUANMING (1995): Site preference of rare earth elements in fluorapatite. *Am. Mineral.* **80**, 329-335.
- FRANZ, L., BECKER, K.-P., KRAMER, W. & HERZIG, P.M. (2002): Metasomatic mantle xenoliths from the Bismarck microplate (Papua New Guinea) – thermal evolution, geochemistry and extent of slab-induced metasomatism. *J. Petrol.* **43**, 315-343.
- GRICE, J.D., SZYMAŃSKI, J.T. & JAMBOR, J.L. (1996): The crystal structure of clinoatacamite, a new polymorph of $\text{Cu}_2(\text{OH})_3\text{Cl}$. *Can. Mineral.* **34**, 73-78.
- HANNINGTON, M.D. (1993): The formation of atacamite during weathering of sulfides on the modern seafloor. *Can. Mineral.* **31**, 945-956.
- HAWTHORNE, F.C. (1985): Refinement of the crystal structure of botallackite. *Mineral. Mag.* **49**, 87-89.
- _____ & GROAT, L.A. (1985): The crystal structure of wroewolfeite, a mineral with $[\text{Cu}_4(\text{OH})_6(\text{SO}_4)(\text{H}_2\text{O})]$ sheets. *Am. Mineral.* **70**, 1050-1055.
- HERZIG, P. M., HANNINGTON, M. D., MCINNES, B., STOFFERS, P., VILLINGER, H., SEIFERT, R., BINNS, R., LIEBE, T. & SCIENTIFIC PARTY R.V. SONNE CRUISE SO-94 (1994): Submarine volcanism and hydrothermal venting studied in Papua New Guinea. *Trans. Am. Geophys. Union (Eos)* **75**, 513-516 (abstr.).
- _____, _____, STOFFERS, P., BECKER, K.-P., DRISCHEL, M., FRANKLIN, J., FRANZ, L., GEMMEL, J. B., HOEPPNER, B., HORN, C., HERZ, K., JELLINECK, T., JONASSON, I. R., KIA, P., NICKELSEN, S., PERCIVAL, J., PERFIT, M., PETERSEN, S., SCHMIDT, M., SEIFERT, T., THIESSEN, O., TÜRKAY, M., TUNNICLIFFE, V. & WINN, K. (1998): Petrology, gold mineralization and biological communities at shallow submarine volcanoes of the New Ireland fore-arc (Papua New Guinea): preliminary results of R/V Sonne cruise SO-133. *Inter Ridge News* **7**, 34-38.
- IRVINE, T.N. (1982): Terminology for layered intrusions. *J. Petrol.* **23**, 127-162.
- JAMBOR, J.L., DUTRIZAC, J.E., ROBERTS, A.C., GRICE, J.D. & SZYMAŃSKI, J.T. (1996): Clinoatacamite, a new polymorph of $\text{Cu}_2(\text{OH})_3\text{Cl}$ and its relationship to paracamite and "anarakite". *Can. Mineral.* **34**, 61-72.
- JOYCE, D.B. & HOLLOWAY, J.R. (1993): An experimental determination of the thermodynamic properties of $\text{H}_2\text{O}-\text{CO}_2-\text{NaCl}$ fluids at high pressures and temperatures. *Geochim. Cosmochim. Acta* **75**, 733-746.
- KAMENETSKY, V.S., DAVIDSON, P., MERNAGH, T.P., CRAWFORD, A.J., GEMMEL, J.B., PORTNYAGIN, M.V. & SHINJO, R. (2002): Fluid bubbles in melt inclusions and pillow-rim glasses: high-temperature precursors to hydrothermal fluids? *Chem. Geol.* **183**, 349-364.

- KENNEDY, A.K., HART, S.R. & FREY, F.A. (1990): Composition and isotopic constraints on the petrogenesis of alkaline arc lavas, Lihir Island, Papua New Guinea. *J. Geophys. Res.* **95**, 6929-6942.
- LEAKE, B.W., WOOLLEY, A.R., ARPS, C.E.S., BIRCH, W.D., GILBERT, M.C., GRICE, J.D., HAWTHORNE, F.C., KATO, A., KISCH, H.J., KRIVOVICHEV, V.G., LINTHOUT, K., LAIRD, J., MANDARINO, J., MARESCH, W.V., NICKEL, E.H., ROCK, N.M.S., SCHUMACHER, J.C., SMITH, D.C., STEPHENSON, N.C.N., UNGARETTI, L., WHITTAKER, E.J.W. & GUO, YOUZHI (1997): Nomenclature of amphiboles. Report of the subcommittee on amphiboles of the International Mineralogical Association Commission on New Minerals and Mineral Names. *Eur. J. Mineral.* **9**, 623-651.
- LEBEDEV, L.M. (1983): Cheleken hydrothermal system – a natural mineral forming laboratory. *Izv. Akad. Nauk SSSR, Ser. Geol.* **7**, 60-75 (in Russ.).
- LE MAITRE, R.W., ed. (2002): *Igneous rocks. A Classification and Glossary of Terms; Recommendations of the International Union of Geological Sciences, Subcommission on the Systematics of Igneous Rocks*. Cambridge University Press, Cambridge, U.K.
- LOWENSTERN, J.B. (1993): Evidence for a copper-bearing fluid in magma erupted at the Valley of Ten Thousand Smokes, Alaska. *Contrib. Mineral. Petrol.* **114**, 409-421.
- _____ (1994): Chlorine, fluid immiscibility and degassing in peralkaline magmas from Pantelleria, Italy. *Am. Mineral.* **79**, 353-356.
- _____ (2000): A review of the contrasting behavior of two magmatic volatiles: chlorine and carbon dioxide. *J. Geochem. Explor.* **69-70**, 287-290.
- _____, MAHOOD, G.A., RIVERS, M.L. & SUTTON, S.R. (1991): Evidence for extreme partitioning of copper into a magmatic vapor phase. *Science* **252**, 1405-1409.
- MCINNIS, B.I.A. & CAMERON, E.M. (1994): Carbonated, alkaline metasomatic melts from a sub-arc environment: mantle wedge samples from the Tabar – Lihir – Feni arc, Papua New Guinea. *Earth Planet. Sci. Lett.* **122**, 125-141.
- _____, GREGOIRE, M., BINNS, R.A., HERZIG, P.M. & HANNINGTON, M.D. (2001): Hydrous metasomatism of oceanic sub-arc mantle, Lihir, Papua New Guinea: petrology and geochemistry of fluid-metasomatized mantle wedge xenoliths. *Earth Planet. Sci. Lett.* **188**, 169-183.
- _____, MCBRIDE, J.S., EVANS, N.J., LAMBERT, D.D. & ANDREW, A.S. (1999): Osmium isotope constraints on ore metal recycling in subduction zones. *Science* **286**, 512-517.
- METRICH, N. & RUTHERFORD, M.J. (1992): Experimental study of chlorine behavior in hydrous silicic melts. *Geochim. Cosmochim. Acta* **56**, 607-616.
- MILLS, R.A., CLAYTON, T. & ALT, J.C. (1996): Low-temperature fluid flow through sulfidic sediments from TAG: modification of fluid chemistry and alteration of mineral deposits. *Geophys. Res. Lett.* **23**, 3495-3498.
- MOENKE, H. (1966): *Mineralspektren*. Akademie Verlag, Berlin, Germany.
- MOYLE, A.J., DOYLE, B.J., HOOGVLIET, H. & WARE, A.R. (1990): Ladolam gold deposit, Lihir Island. In *Geology of the Mineral Deposits of Australia and Papua New Guinea* (E.F. Hughes, ed.). The Australasian Institute of Mining and Technology, Melbourne, Australia (1793-1805).
- MÜLLER, D., FRANZ, L., PETERSEN, S., HERZIG, P.M. & HANNINGTON, M. (2003): Comparison of magmatic activity and gold mineralization at Conical Seamount and Lihir Island, Papua New Guinea. *Mineral. Petrol.* **79**, 259-283.
- PARISE, J.B. & HYDE, B.G. (1986): The structure of atacamite and its relationship to spinel. *Acta Crystallogr.* **C42**, 1277-1280.
- PHILPOTTS, A.R. (1982): Compositions of immiscible liquids in volcanic rocks. *Contrib. Mineral. Petrol.* **80**, 201-218.
- _____ (1990): *Principles of Igneous and Metamorphic Petrology*. Prentice Hall, Upper Saddle River, New Jersey.
- POLLARD, A.M., THOMAS, R.G. & WILLIAMS, P.A. (1989): Synthesis and stabilities of the basic copper(II) chlorides atacamite, parataacamite, and botallackite. *Mineral. Mag.* **53**, 557-563.
- RAGONE, V. & OTTONE, G. (1997): Cinque anni di ricerche mineralogiche al Somma – Vesuvio (Napoli). *Riv. Mineral. Ital.* **2**, 137-154.
- RIGHTER, K. & CARMICHAEL, I.S.E. (1996): Phase equilibria of phlogopite lamprophyres from western Mexico: biotite-liquid equilibria and P-T estimates for biotite-bearing igneous rocks. *Contrib. Mineral. Petrol.* **123**, 1-21.
- RUAYA, J.R. & SEWARD, T.M. (1986): The stability of chlorozinc(II) complexes in hydrothermal solutions up to 350°C. *Geochim. Cosmochim. Acta* **50**, 651-661.
- RYTUBA, J.J., MCKEE, E.H. & COX, D. (1993): Geochronology and geochemistry of the Ladolam gold deposit, Lihir Island, and gold deposits and volcanoes of Tabar and Tatau, Papua New Guinea. *U.S. Geol. Surv., Bull.* **2039**, 119-126.
- SCHIANO, P., CLOCCHIATTI, R., SHIMIZU, N., MAURY, R.C., JOCHUM, K.P. & HOFMANN, A.W. (1995): Hydrous, silica-rich melts in the sub-arc mantle and their relationship with erupted arc magmas. *Nature* **377**, 595-600.
- SERAFIMOVA, E.K., SEMENOVA, T.F. & SULIMOVA, N.V. (1994): The copper and lead minerals from ancient fumarole fields of mountain 1004 (Kamchatka). *Vulkanol. Seismol.* **3**, 35-49 (in Russ.).
- SHARKEY, J.B. & LEWIN, S.Z. (1971): Conditions governing the formation of atacamite and parataacamite. *Am. Mineral.* **56**, 181-194.

- _____ & _____ (1972): Thermochemical properties of the copper(II) hydroxychlorides. *Thermochimica Acta* **3**, 189-201.
- SIGNORELLI, S. & CARROLL, M.R. (2000): Solubility and fluid-melt partitioning of Cl in hydrous phonolitic melts. *Geochim. Cosmochim. Acta* **64**, 2851-2862.
- SOURIRAJAN, S. & KENNEDY, G.C. (1962): The system H₂O–NaCl at elevated temperatures and pressures. *Am. J. Sci.* **260**, 115-141.
- STOIBER, R.E. & ROSE, W.I., JR. (1973): Sublimates at volcanic fumaroles of Cerro Negro Volcano, Nicaragua. *Inst. Centroam. Invest. Tecnol. Ind. Publ. Geol.* **4**, 63-67.
- STRACKE, A. & HEGNER, E. (1998): Rifting-related volcanism in an oceanic post-collisional setting: the Tabar – Lihir – Tanga – Feni (TLTF) island chain, Papua New Guinea. *Lithos* **45**, 545-560.
- TAYLOR, B. (1979): Bismarck Sea: evolution of a back arc basin. *Geology* **7**, 171-174.
- WALLACE, P. & CARMICHAEL, I.S.E. (1992): Sulfur in basaltic magmas. *Geochim. Cosmochim. Acta* **56**, 1863-1874.
- WEBSTER, J.D. (1997): Chloride solubility in felsic melts and the role of chloride in magmatic degassing. *J. Petrol.* **38**, 1793-1807.
- WITZKE, T. (1996): Minerale der brennende Halden des "Deutschlandschachtes" in Oelsnitz bei Zwickau, Sachsen, Deutschland. *Aufschluss* **47**, 41-48.
- YANG, K. & SCOTT, S.D. (1996): Possible contribution of a metal-rich magmatic fluid to a sea-floor hydrothermal system. *Nature* **383**, 420-423.

Received January 11, 2003, revised manuscript accepted February 21, 2004.

APPENDIX: SAMPLES AND METHODS

Sample 54GTV2P was recovered from the TUBAF Seamount with a video-guided grab during cruise SO-133 with the research vessel R.V. Sonne. Three polished thin sections of the xenolith were made for petrographic and micro-analytical studies. The host rock was powdered in an agate mill after removing alteration crusts and analyzed for major and trace elements by standard X-ray fluorescence (XRF) analysis at the Institute of Mineralogy of the Freiberg University (K.-P. Becker, analyst). Back-scattered electron (BSE) and secondary electron (SE) scanning electron microscopy was carried out using a JEOL-SEM at Freiberg University. Analyses of mineral and glass were performed using a JEOL JXA-8900R electron microprobe with five spectrometers. Concentrations of the major elements in the silicate minerals were determined at an acceleration voltage of 15 kV and a beam current of 20 nA, with counting times of 20 s for Si, Al, Mg, Ca, Sr, Ba and K, and 30 s for Fe, Na, Cr, Mn and Ti. The silicate glass was analyzed at the same conditions with counting times of 30 seconds (for Si, Al, Mg, Ca, K, Fe), 60 seconds (for Ba, Cl, Cr, Mn, Ti) and 20 seconds (for Na with a defocused beam). The beam diameter ranged between 5 μm for the silicates and 20 μm for the glass phases. The glass was analyzed for sulfur separately at 15 kV, 5 nA and 100 s counting time. The sulfide minerals were analyzed using an acceleration voltage of 20 kV, a beam current of 15 nA, and a defocused beam with a diameter of 25 μm . The Cu₂(OH)₃Cl phase was analyzed at an acceleration voltage of 25 kV and a beam current between 8

and 15 nA to avoid decomposition of the material. Standard reference materials from MACTM (Micro-Analysis Consultants Ltd., U.K.) were used for reference. For the Cl in the salt hydrates, we used both tugtupite and halite as reference material. The (O + H) values were computed by difference from 100%, which seems reasonable because no other anion complexes (e.g., carbonate, sulfate, nitrate or phosphate) was detected by Fourier-transform infrared (FTIR) spectroscopy. X-ray-diffraction analyses were performed at the RWTH Aachen using a Siemens D-500 diffractometer. Owing to the small amount of material available, small isolated grains were mounted on a silicon sample holder and measured in step-scan mode, 0.02° step size, 8 s measuring time per step. CuK α radiation, 35 kV, 45 mA. Infrared spectroscopy measurements were performed using a BioRAD FTS 40 FTIR spectrometer coupled to a UMA-400 FTIR microscope at the Institute of Mineralogy of Freiberg University. We measured single crystals of the Cu₂(OH)₃Cl phase mounted on a ZnSe holder and KBr powder tablets with a resolution of 4 cm⁻¹. The spectral range for the single-crystal measurements covered between 600 and 400 cm⁻¹, and for the tablets, between 400 and 4000 cm⁻¹. The ⁴⁰Ar / ³⁹Ar age determination on hornblende was performed by Geochron Laboratories (Cambridge, Massachusetts, U.S.A.). Hand-picked crystals of magnesiostastite were heated in a resistance furnace, and gas was extracted at 700, 800, 900, 1000, 1200, 1400, 1600 and 1823 K for isotopic measurements of the argon fraction.